# Liquid metallic hydrogen and the structure of brown dwarfs and giant planets

W.B. Hubbard, T. Guillot, J.I. Lunine
*Lunar and Planetary Laboratory, University of Arizona, Tucson, AZ 85721*
hubbard@lpl.arizona.edu

A. Burrows
*Departments of Physics and Astronomy, University of Arizona, Tucson, AZ 85721*

D. Saumon
*Department of Physics and Astronomy, Vanderbilt University, Nashville, TN 37235*

M.S. Marley
*Department of Astronomy, New Mexico State University, Las Cruces, NM 88003*

R.S. Freedman
*Sterling Software, NASA Ames Research Center, Moffett Field, CA 94035*

## ABSTRACT

Electron-degenerate, pressure-ionized hydrogen (usually referred to as metallic hydrogen) is the principal constituent of brown dwarfs, the long-sought objects which lie in the mass range between the lowest-mass stars (about eighty times the mass of Jupiter) and the giant planets. The thermodynamics and transport properties of metallic hydrogen are important for understanding the properties of these objects, which, unlike stars, continually and slowly cool from initial nondegenerate (gaseous) states.

Within the last year, a brown dwarf (Gliese 229 B) has been detected and its spectrum observed and analyzed, and several examples of extrasolar giant planets have been discovered. The brown dwarf appears to have a mass of about forty to fifty Jupiter masses and is now too cool to be fusing hydrogen or deuterium, although we predict that it will have consumed all of its primordial deuterium. This paper reviews the current understanding of the interrelationship between its interior properties and its observed spectrum, and also discusses the current status of research on the structure of giant planets, both in our solar system and elsewhere.

**PACS numbers:** 95.30.Q, 97.82, 96.30.K, 81.30.B

## I. INTRODUCTION

For the purposes of this paper, we define a giant planet to be a hydrogen-rich object similar to Jupiter (mass $M_J = 1.9 \times 10^{30}$ g $= 0.95 \times 10^{-3} M_\odot$, where $M_\odot$ is the solar mass) or Saturn (mass $M_S = 0.3 M_J$), excluding smaller objects similar to Uranus or Neptune which have only small mass fractions of hydrogen. We also define a brown dwarf to be an object with mass smaller than the minimum mass required for sustained thermonuclear fusion of hydrogen (about 85 $M_J$), but larger than the minimum mass required for fusion of deuterium (about 13.5 $M_J$). In fact the latter distinction is somewhat arbitrary, for giant planets and brown dwarfs constitute a seamless continuum, with the same interior physics applying to both.

There has long been a wealth of theoretical studies of the properties of giant planets and brown dwarfs[1,2], but prior to 1995, the only objects to which these theories could be applied were Jupiter and Saturn. However, the year 1995 marked an explosive turning point in this situation. Within an interval of a few months, the first detections of extrasolar giant planets were reported[3], and a bona fide brown dwarf, Gl229 B, was discovered[4]. In rapid succession, high-quality spectral data on the emissions of the new brown dwarf were obtained, permitting an initial determination of its atmospheric composition[5], and an entry probe carried out *in situ* measurements of the structure and composition of the Jovian atmosphere to a pressure of 20 bars[6]. At the same time, developments in high-pressure technology have allowed new experimental studies of hydrogen in the megabar pressure range[7], and developments in high-pressure theory have given new information about possible phase transitions in hydrogen in the relevant pressure range[8].

Interpretations of the new data are dependent upon, and potentially bear information about, the phase diagram and thermodynamic properties of liquid metallic hydrogen at temperatures $T$ of $\sim 10^4$ to $\sim 10^6$ K, and pressures $P$ of $\sim 1$ to $\sim 10^6$ Mbar. In this paper we consider theoretical interpretations of data for the three main types of objects which relate to the recent observations: (a) brown dwarfs (e.g., Gl229 B); (b) Jupiter; (c) high-temperature giant planets which orbit at small separations from their primary (e.g., 51 Peg B). Our primary focus is upon tests of the hydrogen equations of state and proposed hydrogen phase diagrams.

## II. HYDROGEN PHASE DIAGRAM

The relevant parts of the hydrogen phase diagram are shown in Fig. 1. This diagram is computed assuming pure hydrogen, although, as we shall discuss below, the non-hydrogen components of brown dwarfs and giant planets constitute an important diagnostic for this diagram. The upper-right-hand corner of the experimentally-accessible regime is defined by the open circle, which shows the highest temperature and pressure investigated in recent high-pressure electrical-conductivity experiments[7]. The solid circle shows an experimentally-observed transition to a metallic state of hydrogen at $P = 1.4$ Mbar and $T = 3000$ K. At pressures below the solid circle, electrical conductivity of hydrogen increases rapidly with pressure, while for pressures lying between the two circles, the measured electrical conductivity is essentially constant at 2000 $(\Omega - \mathrm{cm})^{-1}$, but still about two orders of magnitude lower than the value predicted for classical fully-ionized liquid metallic hydrogen at comparable density and temperature. In the experimental data, there is no evidence of a discontinuous change in state as a function of pressure up to the maximum pressure. These data[7] indicate that hydrogen dissociates continuously from the molecular to the metallic phase with no first-order transition. Furthermore, the gradual latent heat release associated with the gradual dissociation causes a cooling effect on interior temperatures similar to the effect of a radiative zone in Jupiter and cooler brown dwarfs described below. A fully self-consistent equation of state for models of these objects which fully incorporates the new experimental data is not yet available.

The conductivity measurements bear upon theoretical calculations of the hydrogen phase diagram at temperatures near $10^4$ K and pressures $\sim 0.1$ to 1 Mbar. Figure 1 shows two such caculations, which have qualitatively similar results, predicting that a phase transition exists between two liquid phases of hydrogen. The calculation by Saumon *et al.*[8] is based upon a chemical approach which evaluates the equilibrium between various neutral and ionized forms of H and $H_2$, while the calculation by Magro *et al.*[8] is based upon first-principles evaluation of the quantum partition function of a system of electrons and protons. Both calculations

predict a critical point at a temperature slightly above $10^4$ K and a pressure somewhat below 1 Mbar, but neither extend into the range where electrical conductivity was measured. In this connection it should be mentioned that shock-compression experiments up to $T = 5200$ K and $P = 0.83$ Mbar show no evidence of a major discontinuity in density, although a small discontinuity ($\lesssim$10%) could remain undetected[7].

Also shown in Fig. 1 is the experimentally-observed boundary between liquid and solid phases of $H_2$, extrapolated to $P \approx 1.4$ Mbar[9], and the theoretically-calculated boundary between liquid and solid phases of classical metallic hydrogen[10], assuming that the transition occurs at a proton plasma coupling parameter $\Gamma = 175$, and making no correction for electron screening or quantum oscillations of the protons (both of which will lower the melting temperature). Vertical dashed lines show guesses for the possible behavior of the boundary between the insulating and metallic liquid phases (upper dashed line) and the insulating and metallic solid phases (lower dashed line). As we shall see, neither solid phase is relevant to astrophysical objects.

Finally, at the top of Fig. 1 we show the locus of central points in brown-dwarf models where 50% of the luminosity is derived from thermonuclear conversion of deuterium nuclei to $^3$He nuclei; for objects which achieve central temperatures above this line, all of the deuterium is consumed during the first $\sim 0.01$ Gyr of the objects' existence[11]. The dot marking the end of this locus shows the center of a critical model which is just able to ignite deuterium fusion. This occurs under conditions of intermediate proton (deuteron) coupling with $\Gamma \approx 2$.

## III. EVOLUTIONARY SEQUENCES

The region of the hydrogen phase diagram which is probed by evolving giant planets and brown dwarfs is shown in Fig. 2. This figure shows, on the same plane as Fig. 1, calculated $T$ vs. $P$ profiles for the interior of Jupiter (shorter lines) and the interior of Gl229 B (longer lines), at various ages. The profiles are isentropes calculated for a solar mixture of hydrogen and helium (28 % helium by mass), using the Saumon-Chabrier-Van Horn (SCVH) equation of state[8]. For objects in this mass range, the interior is maintained in a state of efficient convection by virtue of the relatively low thermal conductivity of metallic hydrogen and the relatively high opacity of molecular and metallic hydrogen (with the exception of a radiative zone which appears in Jupiter and in cooler brown dwarfs at temperatures between 1200 and 2900 K)[12]. As a result the temperature profile remains close to an isentrope throughout the interior, with the specific entropy defined by the radiative properties of the optically-thin outer layers.

The evolution of a giant planet or brown dwarf is calculated by using a relation of the form $S/N = f(T_{\rm eff}, g)$, where $S/N$ is the specific entropy (entropy per nucleon), $T_{\rm eff}$ is the effective temperature of the atmosphere, and $g$ is the surface gravity. Calculation of $f$ involves solution of the coupled equations of radiative/convective heat transport and hydrostatic equilibrium for specified $T_{\rm eff}$ and $g$ in the relevant ranges ($T_{\rm eff} = 124$ K and $g = 23$ m/s$^2$ for Jupiter, to $T_{\rm eff} = 960$ K and $g = 1000$ m/s$^2$ for Gl229 B), and is nontrivial, as atmospheres in the relevant ranges have extremely nongrey fluxes (for Gl229 B the predicted fluxes vary by as much as three orders of magnitude over adjacent wavelength bands), and trace species such as methane, water, and ammonia have major influences on the fluxes. Mapping of the function $f$ over the relevant $T_{\rm eff}, g$ range is still in progress, but initial results[11] have been obtained for the evolution of objects in the mass range from $\sim 80\ M_J$ down to $\sim 1\ M_J$.

The first general calculation of the evolution of giant planets and brown dwarfs was carried out by Black[13], who fitted power laws to existing calculations for the evolution of Jupiter and brown dwarfs, and used the results to predict the behavior of objects in the range from $\sim 1$ to $15\ M_J$. Saumon *et al.*[11] improved upon this calculation by using quantitative theories for the interior thermodynamics and thermonuclear reaction rates of metallic-hydrogen liquids, and interpolating in a grid of values for $f$ for Jovian and near-Jovian $T_{\rm eff}, g$ in the low end, and previously-calculated values for brown dwarfs with grey model atmospheres with $M > 15 M_J$ at the high end. Some sample results from the latter calculation are shown in Fig. 3. This figure displays the radii of giant planets as a function of their mass for logarithmically-equal time intervals from an age $t = 10^{-3}$ Gyr to 4.6 Gyr (present age of Jupiter). As is well known, the compressibility of liquid metallic hydrogen is such that an approximately constant radius

of around $10^5$ km is maintained throughout the indicated mass and age range. For fixed age, a minimum radius (at mass $M = 2\ M_J$) at about 120000 km at $t = 10^{-3}$ Gyr is replaced by a maximum radius at about 78000 km, slightly larger than Jupiter's present radius, at mass $M = 4\ M_J$ and $t = 4.6$ Gyr.

With the discovery of Gl229 B and the availability of a high-quality spectrum of this object, it has become imperative to generate nongrey model atmospheres to fit the observations, and to simultaneously use the atmospheres to determine the best-fit values of $T_{\rm eff}, g$ and thus $f$.

Figure 4 shows a best-fit model generated by our group for the atmospheric profile of $T$ vs. $P$ in Gl229 B, along with a comparison profile for Jupiter[5]. At higher pressures (about 40 bar for Gl229 B and 0.4 bar for Jupiter), the profile merges with an isentrope (dashed line), the continuation of which is shown in Fig. 2 (lowest profile for each object).

Our updated grid of $f$ values, using the optimized $T(P)$ profiles which best fit the Gl229 B spectrum, was used to generate an evolutionary sequence. A summary of the results is presented in Fig. 5. It turns out that at the present stage of fitting Gl229 B's spectrum, the value of $g$ is only poorly constrained, while $T_{\rm eff}$ is better determined. We find that Gl229 B fits the theory for brown dwarfs extremely well, and there can be no doubt that this object is a member of the class. The interior $T(P)$ profiles shown in Fig. 2 correspond to a likely model inferred from Fig. 5, with a mass of 40 $M_J$ and an age of 1.7 Gyr. It is noteworthy that the isentrope corresponding to the present Gl229 B is very close to the Jovian isentrope calculated for a Jovian age of $\sim 0.1$ Gyr, but of course extends to a central pressure four orders of magnitude larger. Because the central pressure and temperature of Gl229 B greatly exceed the limit for deuterium fusion, no primordial deuterium should be present in this brown dwarf's atmosphere.

The interior isentrope corresponding to a jovian planet of $M \sim 1\ M_J$ heated to $T_{\rm eff} \approx 1250$ K by close proximity to a primary star (e.g., 51 Peg B), at an age of 8 Gyr, turns out to be very similar to a Jovian adiabat at an age of 1 Gyr (see Fig. 2). A high-temperature outer radiative zone is created by the insolation from the primary, but this involves only a small fraction of the planet's mass and radius[14]. Because the interior of the planet is at a much higher entropy at an age of 8 Gyr, the planet is significantly thermally expanded in radius (by $\sim 20$ %) compared with the present Jupiter. Nevertheless a high-temperature jovian planet similar to 51 Peg B, orbiting at only 0.05 A.U. from its primary, is quite stable.

## IV. IMPLICATIONS FOR ATMOSPHERIC ABUNDANCES

Figure 6 shows the phase diagram of Fig. 1 combined with the evolutionary trajectories of Fig. 2. The principal implications of this figure are as follows. If a high-temperature first-order phase transition exists between two liquid phases of hydrogen (the so-called plasma phase transition, or PPT), then according to the Gibbs phase rule, in thermodynamic equilibrium the concentrations of nonhydrogen species such as noble gases, water, methane, etc., cannot be continuous across the boundary. This mechanism for affecting the atmospheric abundances of brown dwarfs and giant planets is separate, and possibly in addition to, the proposed limited solubility of such species in metallic hydrogen[2]. As Figure 6 indicates, both Jupiter and brown dwarfs such as Gl229 B will evolve in such a way as to cross the PPT at later stages in their evolution. However, it is interesting to note that at the age that we derive for Gl229 B, it would cross the PPT calculated by Saumon *et al.* but would just miss the critical point of the PPT calculated by Magro *et al.*[8]

We do not know the effect of the PPT on the partitioning of nonhydrogen species, for no one has carried out the requisite calculations. Moreover, an abundant impurity (helium) will significantly shift the location of the PPT as well. In principle one could test for partitioning across the PPT by comparing the atmospheric abundances of objects such as Jupiter and Gl229 B. Water is prominent in the observed spectrum of Gl229 B, has recently been measured in the deep Jovian atmosphere by an entry probe[8], and should if it has solar abundance be present at a number fraction of about $1.5 \times 10^{-3}$ relative to $H_2$. The synthetic spectrum of Gl229 B generated by our group, under the assumption of solar abundance of $H_2O$ in the atmosphere, is a good if not perfect fit to the data[5]. Water opacity dominates many bands of the Gl229 B spectrum, superimposed on a general background opacity provided by pressure-induced dipole transitions of $H_2$. A few bands are indicative of methane and ammonia opacity, which are also presumed to be present in solar abundance. While a quantitative determination of abundances in Gl229 B remains to be done, at this stage it appears to be safe to say that its atmosphere has a solar abundance of C, N, and O.

As in Gl229 B, the C, N, and O in Jupiter's observable atmosphere are primarily in the form of $CH_4$, $NH_3$, and $H_2O$. The first two are readily measurable in the Jovian spectrum, and are found to be enhanced by about a factor of two over solar composition[6]. The *in situ* measurements by the Galileo entry probe are more uncertain because they are still under analysis; Jovian $CH_4$ is found to be present at 2.9 times solar concentration. However, the presently-available interpretation of the probe data suggests that Jupiter's atmospheric $H_2O$ is depleted by about a factor 5 relative to solar[6].

There is a known effect, quite independent of the PPT, which could affect Jupiter's atmospheric water abundance. In Fig. 4 we have indicated the condensation line for $H_2O$ in a solar-composition atmosphere. Above this line, the $H_2O$ is in full concentration in the ambient gas, but below this line, the formation of a condensed phase of $H_2O$ will reduce the gas-phase concentration in accordance with vapor-solid (or liquid) equilibrium. Note that the atmosphere of Gl229 B is everywhere so warm that its $H_2O$ cannot be affected by this process. It was expected that by the time the Galileo probe reached the 20 bar level, the $H_2O$ would be fully in solution in the background gas, so a possible strong depletion at the deepest levels probed would be puzzling. To explain the seeming inconsistency with solar composition, Niemann *et al.* considered various alternative scenarios, including extreme downdrafts which might deplete water in the region entered by the probe[6].

A scenario not considered by Niemann *et al.* is possible partitioning by a PPT. Jupiter's interior isentrope is everywhere much colder than that of Gl229 B. Not only does Jupiter's isentrope lie within the field of $H_2O$ condensation, it also lies deep within the PPT of both current theoretical models for liquid metallic hydrogen (strictly speaking, the "isentrope" would have continuous $T$ and $P$ across the PPT, and discontinuous entropy and composition).

## V. CONCLUSIONS

With the availability of detailed data for the properties and atmospheric abundances of brown dwarfs and jovian planets, it is becoming possible to probe the properties of the phase diagram of hydrogen in the vicinity of the region where dense molecular hydrogen liquid trans-

forms into metallic hydrogen liquid. Earlier work[2] has shown that in the metallic-hydrogen liquid, various impurities such as helium may have limited solubility, and that this may affect atmospheric abundances. Here we point out that, quite apart from possible precipitation within the liquid metallic phase, a first-order phase transition to the metallic phase will affect relative abundances of species regardless of their overall concentration. We are now able to study relative abundances in an object (Gl229 B) which almost certainly lies above or very near any PPT critical point, and objects (Jupiter and Saturn) which lie well below that critical point. Determination of the existence of a PPT in hydrogen has therefore become a first-order priority for the interpretation of new astrophysical data on giant planets and brown dwarfs. If it can be definitively shown to exist through experiment and theory, then determination of the partitioning coefficients for various elements in the two phases will be essential for understanding the interior structure of giant planets and brown dwarfs.

## ACKNOWLEDGMENTS

This work was supported by National Aeronautics and Space Administration grants NAGW-1555 and NAGW-2817, by National Science Foundation grant AST93-18970, and by a European Space Agency fellowship to T.G. and a Hubble Fellowship to D.S.

## REFERENCES


[1] M.S. Kafatos, R.S. Harrington, S.P. Maran, *Astrophysics of Brown Dwarfs* (Cambridge Univ. Press, Cambridge, 1986).

[2] D.J. Stevenson, E.E. Salpeter, Astrophys. J. Suppl. **35**, 221 (1977); ibid, 239.

[3] M. Mayor, D. Queloz, Nature **378**, 355 (1995); G.W. Marcy, R.P. Butler, Astrophys. J. Lett. **464**, L147.

[4] T. Nakajima, B.R. Oppenheimer, S.R. Kulkarni, D.A. Golimowski, K. Matthews, S.T. Durrance, Nature **378**, 463 (1995); B.R. Oppenheimer, S.R. Kulkarni, K. Matthews, T. Nakajima, Science **270**, 1478 (1995).

[5] M.S. Marley, D. Saumon, T. Guillot, R.S. Freedman, W.B. Hubbard, A. Burrows, J.I. Lunine, Science **272**, 1919 (1996).

[6] H.B. Niemann, S.K. Atreya, G.R. Carignan, T.M. Donahue, J.A. Haberman, D.N. Harpold, R.E. Hartle, D.M. Hunten, W.T Kasprzak, P.R. Mahaffy, T.C. Owen, N.W. Spencer, Science **272**, 846 (1996); U. von Zahn, D.M. Hunten, Science **272**, 849 (1996).

[7] S.T. Weir, T. Mitchell, W.J. Nellis, Phys. Rev. Lett. **76**, 1860 (1996); W.J. Nellis, M. Ross, N.C. Holmes, Science **269**, 1249 (1995).

[8] D. Saumon, G. Chabrier, H.M. Van Horn, Astrophys. J. Suppl. **99**, 713 (1995); W.R. Magro, D.M. Ceperley, C. Pierleoni, B. Bernu, Phys. Rev. Lett. **76**, 1240 (1996).

[9] I.F. Silvera, in *Simple Molecular Systems at Very High Density*, edited by A. Polian, P. Loubeyre, and N. Boccara (Plenum, New York, 1989), p. 33.

[10] M.D. Jones, D.M. Ceperley, Phys. Rev. Lett. **76**, 4572 (1996).

[11] D. Saumon, W.B. Hubbard, A. Burrows, T. Guillot, J.I. Lunine, G. Chabrier, Astrophys. J. **460**, 993 (1996).

[12] T. Guillot, G. Chabrier, D. Gautier, P. Morel, Astrophys. J. **450**, 463 (1995).

[13] D.C. Black, Icarus **43**, 293 (1980).

[14] T. Guillot, A. Burrows, W.B. Hubbard, J.I. Lunine, D. Saumon, Astrophys. J. Lett. **459**, L35 (1996).

## FIGURE CAPTIONS

**Fig. 1** – The phase diagram of hydrogen at high pressures and temperatures. Alternate plasma phase transition lines calculated by Magro *et al.* (QMC stands for "quantum Monte Carlo"), and by Saumon *et al.* (SCVH) are shown; both terminate in a critical point[8]. "D burns" is not a phase transition but rather the locus of marginal deuterium thermonuclear fusion under conditions of intermediate plasma coupling.

**Fig. 2** – Interior temperature-pressure profiles for Jupiter and Gl229 B; the age of the object in Gyr is given at the end of each profile. An open box marks the central conditions at each age. A solid triangle shows central conditions for a jovian-planet model of the high-temperature extrasolar planet 51 Peg B.

**Fig. 3** – Radius vs. mass at various ages (equally spaced logarithmically) for jovian planets. Present values for Jupiter (J) and Saturn (S) are shown, along with values for the non-hydrogenic giant planets Uranus (U) and Neptune (N). The observed radii of Jupiter and Saturn are slightly lower than values computed for solar composition because these planets have interiors enriched in elements heavier than hydrogen and helium.

**Fig. 4** – Atmospheric temperature profiles for Gl229 B and Jupiter (solid lines). At higher pressures, these profiles merge with isentropes (short-dashed lines). The long-dashed curve shows the locus of points below which water in a solar-composition atmosphere is in equilibrium with a condensed (liquid or solid) phase.

**Fig. 5** – A plot of surface gravity $g$ vs. effective temperature $T_{\rm eff}$ for brown dwarf models. Constraints on effective temperature and surface gravity of Gl229 B are shown as a shaded central area. Contours of constant mass (in $M_J$), radius (in km), and age (in Gyr) are superimposed.

**Fig. 6** – A superimposition of Figs. 1 and 2, showing positions of Jupiter and Gl229 B evolutionary models with respect to the hydrogen phase diagram.

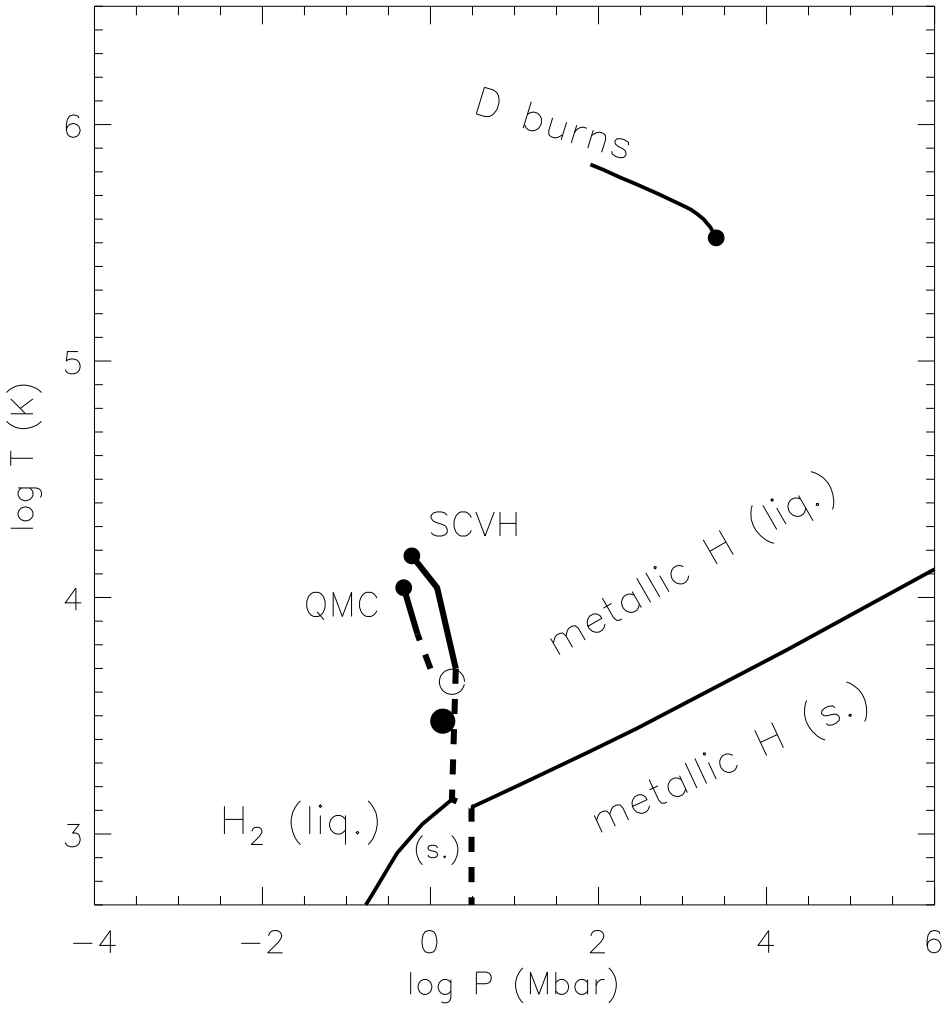
D burns
SCVH
QMC
metallic H (liq.)
metallic H (s.)
H2 (liq.)
(s.)
C
log T (K)
log P (Mbar)
6
5
4
3
−4
−2
0
2
4
6

Fig. 1

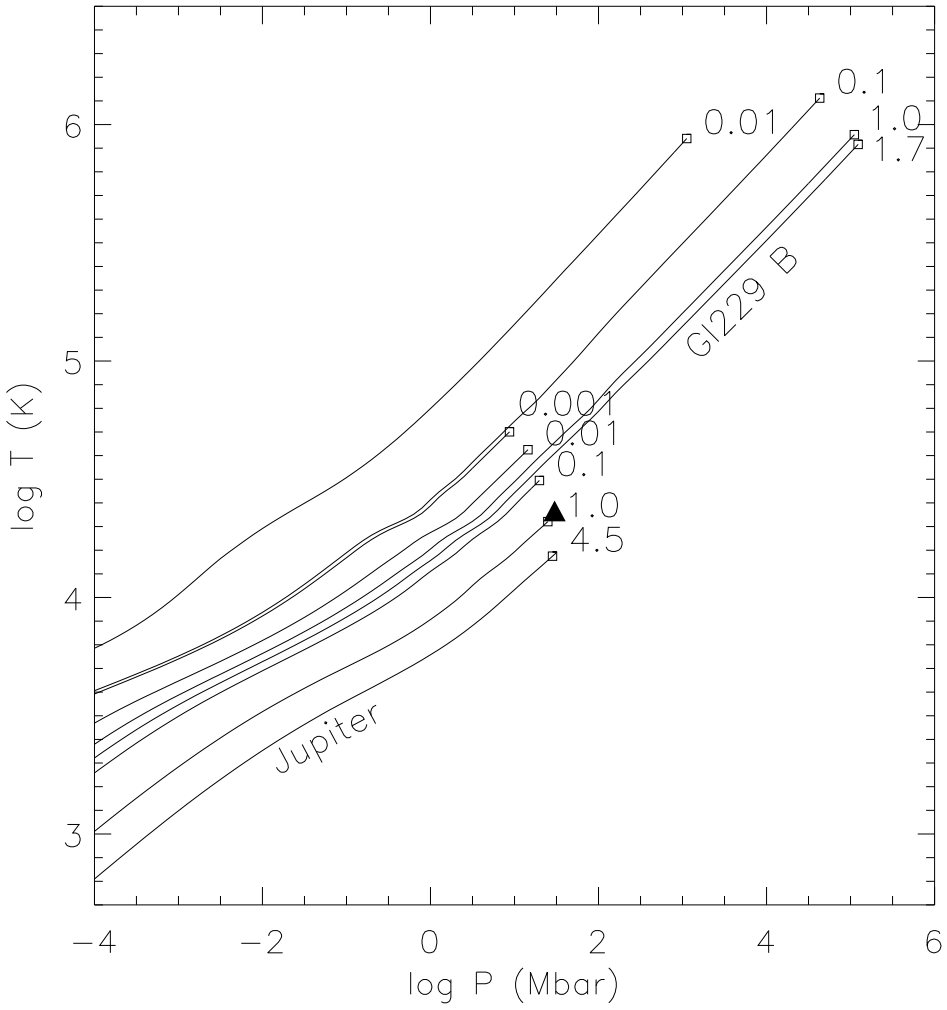
0.1
0.01
1.0
1.7
0.001
0.01
0.1
1.0
4.5
Gl229 B
Jupiter
log T (K)
log P (Mbar)
6
5
4
3
−4
−2
0
2
4
6

Fig. 2

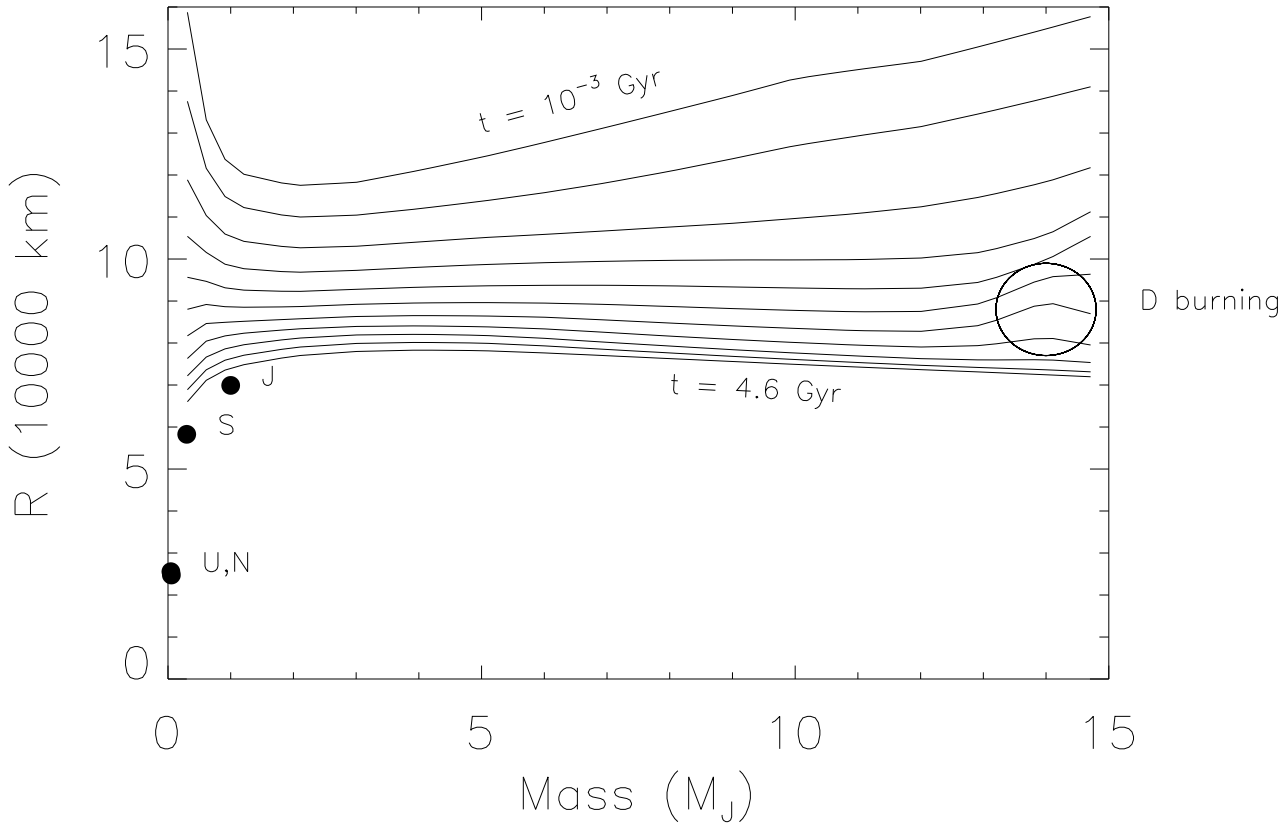
15
10
5
0
R (10000 km)
t = 10^-3 Gyr
t = 4.6 Gyr
D burning
J
S
U,N
0
5
10
15
Mass (M_J)

Fig. 3

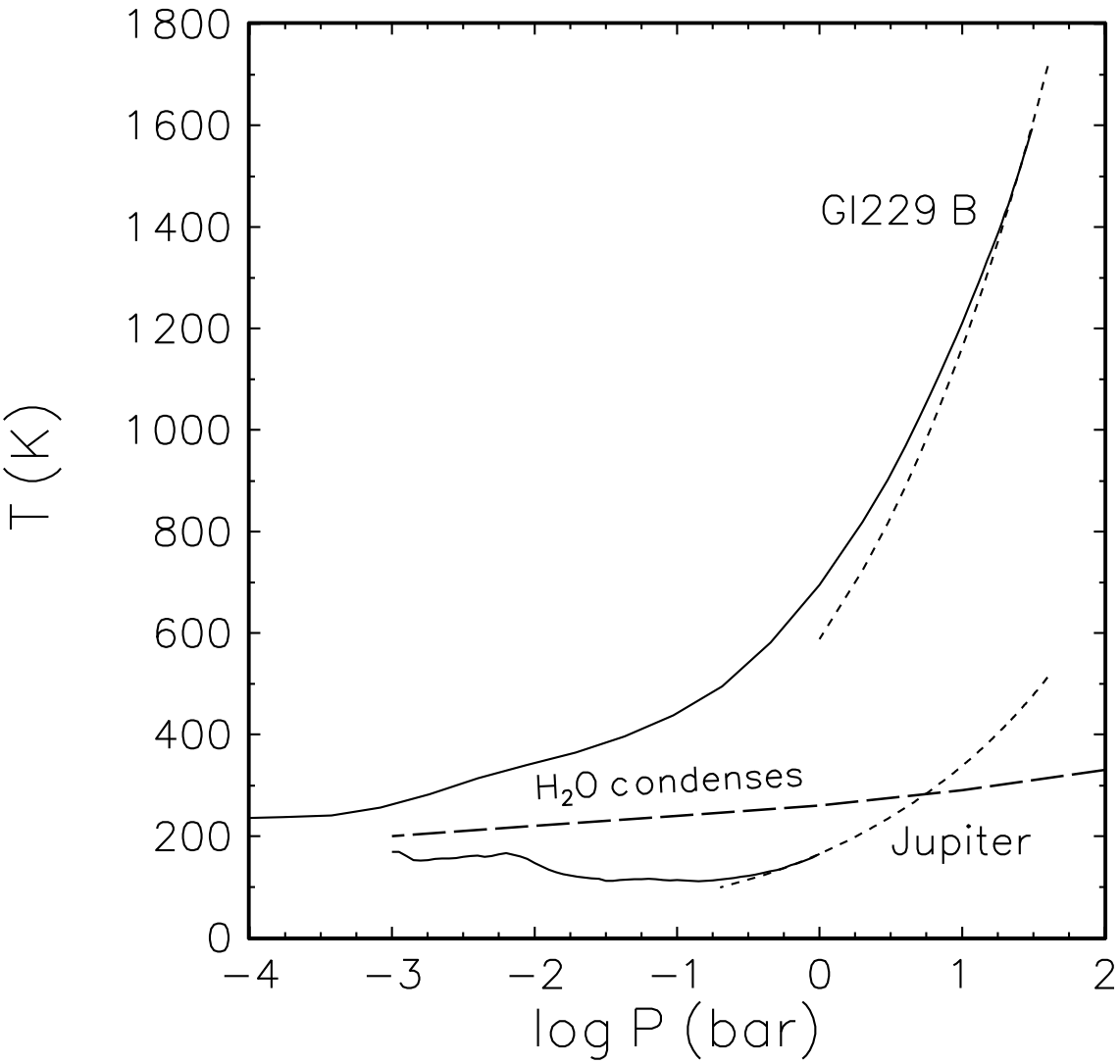
1800
1600
1400
1200
1000
800
600
400
200
0
T (K)
−4
−3
−2
−1
0
1
2
log P (bar)
Gl229 B
H2O condenses
Jupiter

Fig. 4

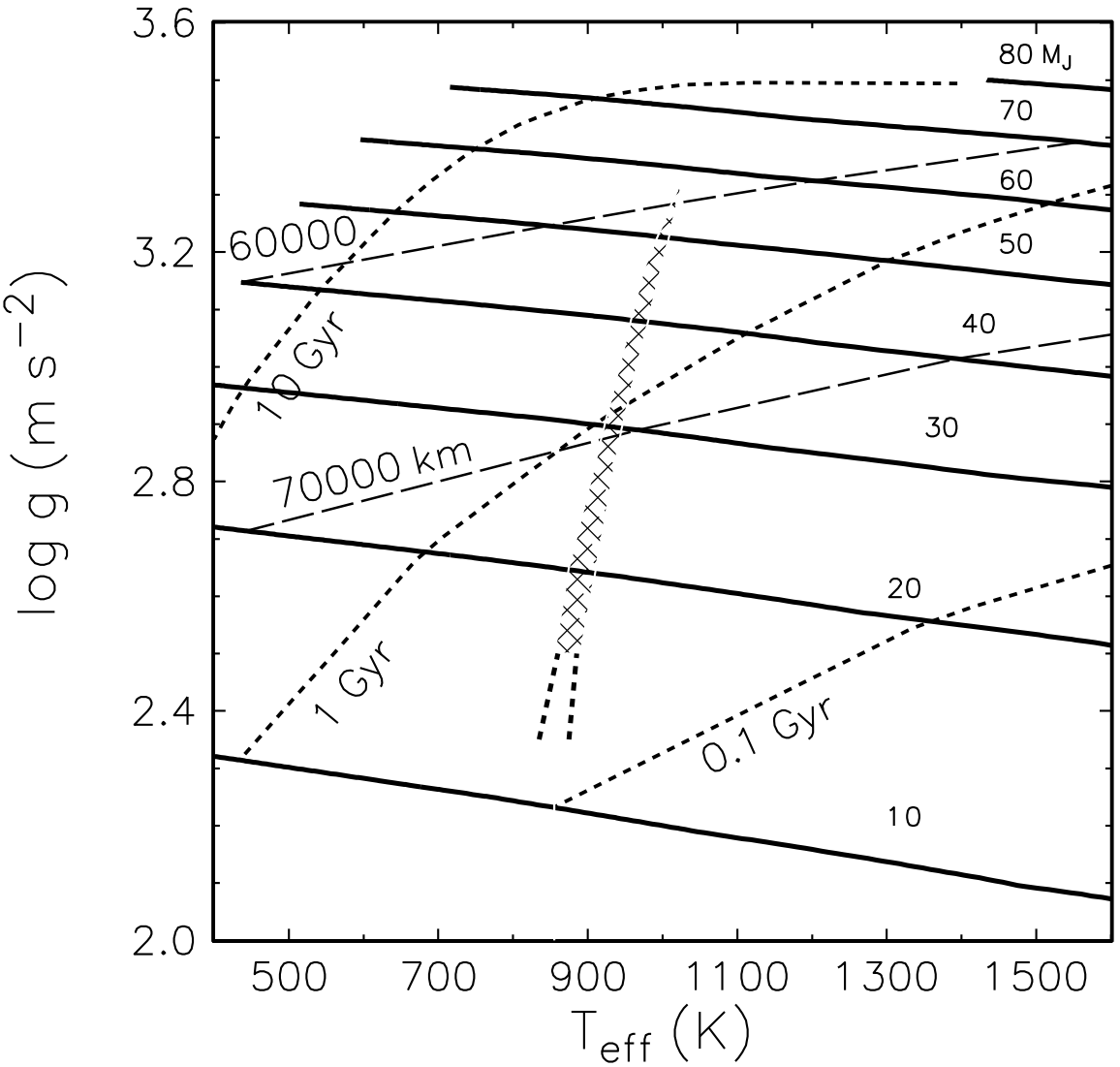
3.6
3.2
2.8
2.4
2.0
log g (m s$^{-2}$)
500
700
900
1100
1300
1500
$T_{eff}$ (K)
80 $M_J$
70
60
50
40
30
20
10
60000
70000 km
10 Gyr
1 Gyr
0.1 Gyr

Fig. 5

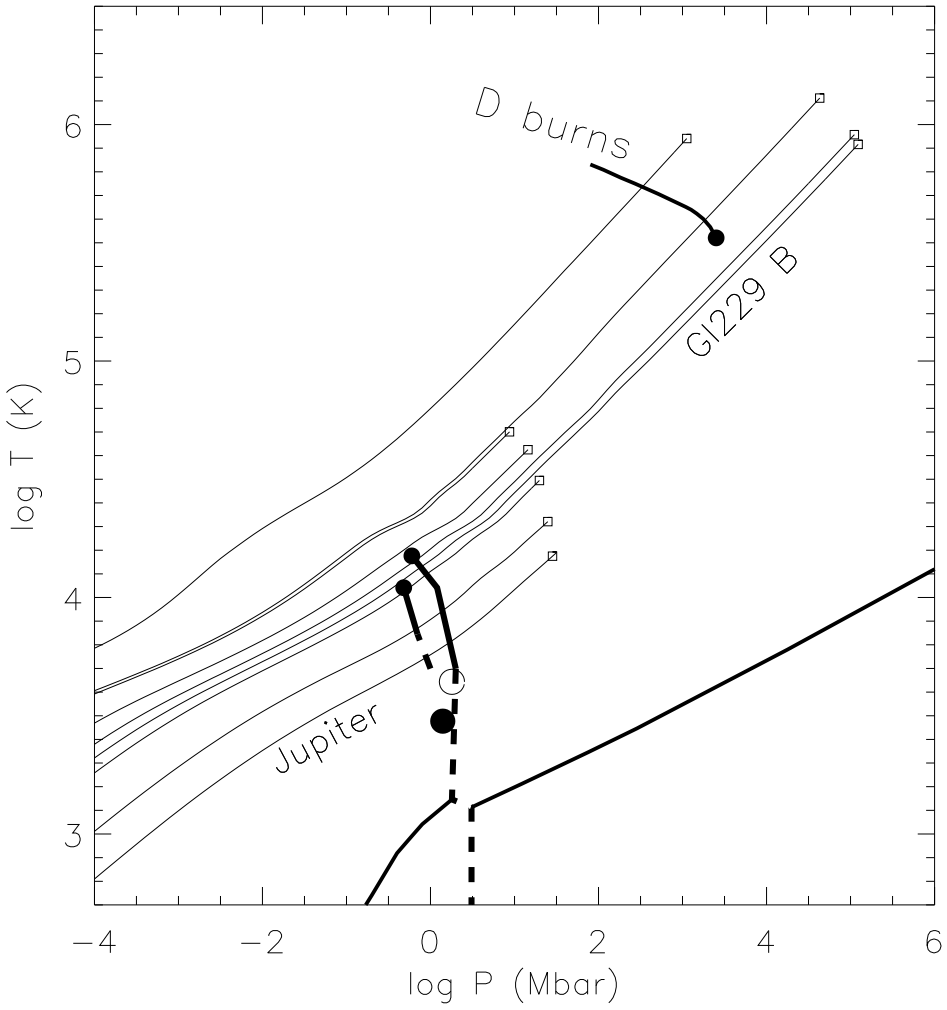


Fig. 6